Volume 6 | Number 5 | May 2014 | Pages 479–578

Integrative Biology

Interdisciplinary approaches for molecular and cellular life sciences

www.rsc.org/ibiology

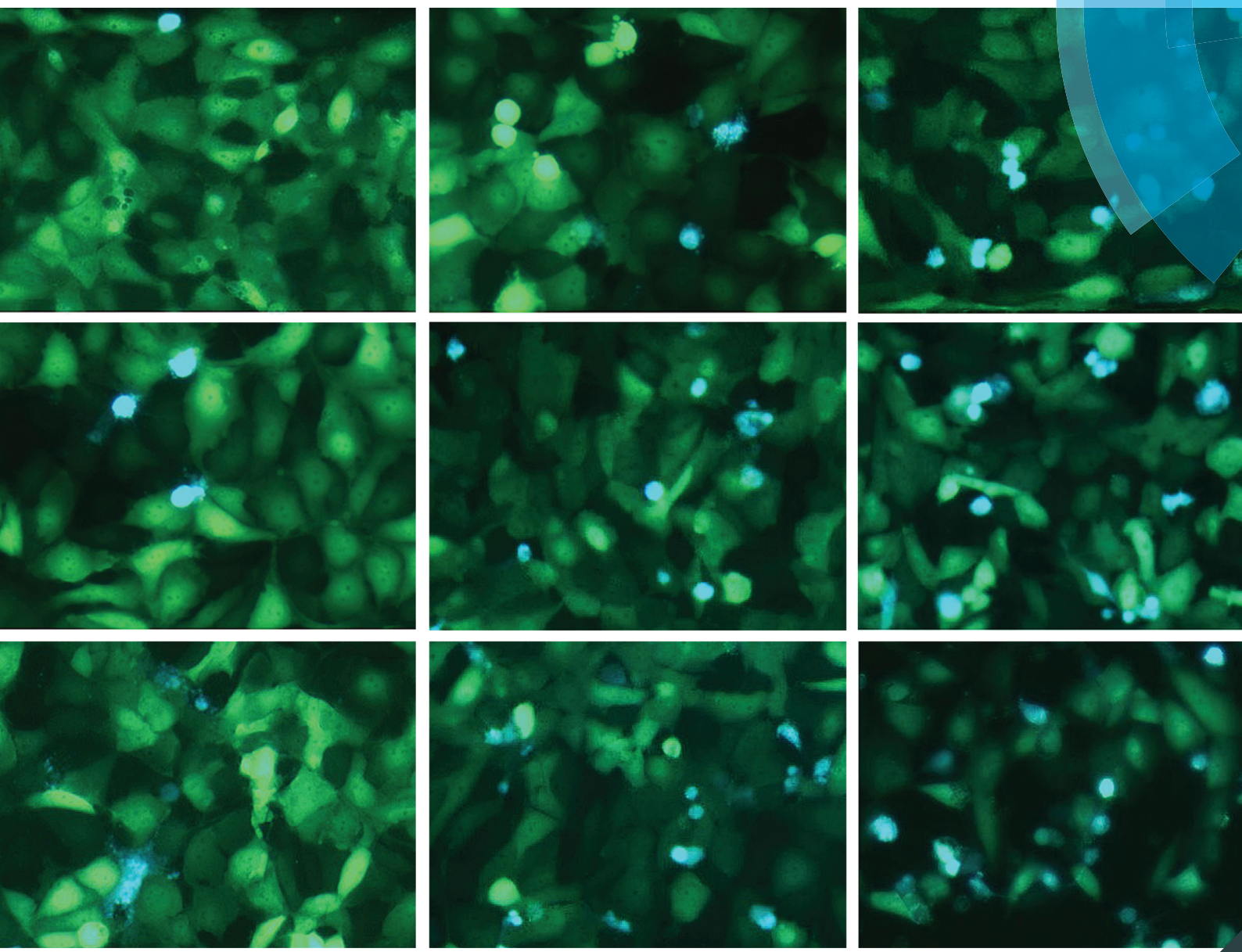

ISSN 1757-9694

ROYAL SOCIETY OF CHEMISTRY

PAPER

K. Q. Luo *et al.*

Biological factors in plasma from diabetes mellitus patients enhance hyperglycaemia and pulsatile shear stress-induced endothelial cell apoptosis

Indexed in Medline!

Integrative Biology

PAPER

View Article Online
View Journal | View Issue

Cite this: *Integr. Biol.*, 2014, 6, 511

Biological factors in plasma from diabetes mellitus patients enhance hyperglycaemia and pulsatile shear stress-induced endothelial cell apoptosis†

X. F. Liu,[a] J. Q. Yu,[b] R. Dalan,[cde] A. Q. Liu[a] and K. Q. Luo*[a]

Received 19th December 2013,
Accepted 23rd February 2014

DOI: 10.1039/c3ib40265g

www.rsc.org/ibiology

People suffering from Diabetes Mellitus (DM) are prone to an array of vascular complications leading to end organ damage. The hallmark of these vascular complications is endothelium dysfunction, which is caused by endothelial cell (EC) apoptosis. Although the endothelial cell (EC) dysfunction induced by hyperglycaemia and fluid shear stress has been studied, the effects of biological factors in the blood of DM patients on EC integrity have not been reported in the *in vitro* models that mimic the physiological pulsatile nature of the vascular system. This study reports the development of a hemodynamic lab-on-a-chip system to investigate this issue. The pulsatile flow was applied to a monolayer of endothelial cells expressing a fluorescence resonance energy transfer (FRET)-based biosensor that changes colour from green to blue in response to caspase-3 activation during apoptosis. Plasma samples from healthy volunteers and DM patients were compared to identify biological factors that are critical to endothelial disruption. Three types of microchannels were designed to simulate the blood vessels under healthy and partially blocked pathological conditions. The results showed that EC apoptosis rates increased with increasing glucose concentration and levels of shear stress. The rates of apoptosis further increased by a factor of 1.4–2.3 for hyperglycaemic plasma under all dynamic conditions. Under static conditions, little difference was detected in the rate of EC apoptosis between experiments using plasma from DM patients and glucose medium, suggesting that the effects of hyperglycaemia and biological factors on the induction of EC apoptosis are all shear flow-dependent. A proteomics study was then conducted to identify biological factors, demonstrating that the levels of eight proteins, including haptoglobin and clusterin, were significantly down-regulated, while six proteins, including apolipoprotein C-III, were significantly up-regulated in the plasma of DM patients compared to healthy volunteers. This hemodynamic lab-on-a-chip system can serve as a high throughput platform to assess the risk of vascular complications of DM patients and to determine the effects of therapeutics or other interventions on EC apoptosis.

Insight, innovation, integration

Hyperglycemia is not the only factor that induces vascular complications of diabetes. Blood components in the plasma are also regulators that increase the risk of diabetic complications. Here, with the aid of a hemodynamic system combining the application of plasma samples from humans with diabetes, we demonstrate that the functions of blood components are all shear stress-dependent. Investigations further focus on plasma proteins, revealing that the effect of haptoglobin, high-density lipoproteins such as clusterin, and low-density lipoproteins such as apolipoprotein C-III are crucial to endothelial cell apoptosis, of which the results under hemodynamic conditions are positively correlated with clinical studies of diabetes. These results will facilitate the discovery of factors that can regulate the effect of plasma proteins under hemodynamic conditions.

Introduction

The prevalence of diabetes mellitus (DM) has increased throughout the world. Vascular complications are the main causes of significant morbidity and mortality in DM. Many studies have suggested that an abnormally high blood glucose concentration (hyperglycaemia) is the primary cause of the development and progression of the complications of DM originating from endothelial

[a] *School of Chemical and Biomedical Engineering, Nanyang Technological University, 70 Nanyang Drive, Singapore 637457. E-mail: kluo@ntu.edu.sg*
[b] *School of Electrical and Electronic Engineering, Nanyang Technological University, 50 Nanyang Avenue, Singapore 639798*
[c] *Department of Endocrinology, Tan Tock Seng Hospital, Singapore 308433*
[d] *Yong Loo Lin School of Medicine, National University of Singapore, Singapore 119228*
[e] *Graduate School of Medicine, Duke-NUS, Singapore 169547*

† Electronic supplementary information (ESI) available. See DOI: 10.1039/c3ib40265g

cell (EC) dysfunction. Hyperglycaemia in DM patients increases the risk of microvascular end-points associated with peripheral neuropathy, nephropathy and retinopathy as well as macrovascular diseases such as atherosclerosis.[1–4] Researchers have identified several mechanisms by which hyperglycaemia damages ECs, including polyol pathway flux,[5] oxidative stress,[6] non-enzymatic glycation and diacylglycerol–protein kinase C (DAG–PKC) activation.[7] The principal mechanism is reactive oxygen species (ROS)-mediated oxidative stress, which is related to PKC-dependent NAD(P)H oxidase activation and the down-regulation of the activity and expression of endothelial nitric oxide synthase (eNOS).[8,9]

Recently, other physiological factors have received more attention, such as increased shear stress. Shear stress in the blood vessels has been reported to be a significant modulator of EC function.[10] Appropriate shear flow is an important factor for the formation of blood vessel structures during early development and for the repair of damaged blood vessels in adults.[11,12] Many studies have indicated that ECs can alter their morphology and function in response to shear stress. These responses are closely related to flow-regulated phenomena such as angiogenesis, vascular remodelling and atherosclerosis.[13,14] Additionally, the pulsatile nature of blood flow plays a critical role in revealing the effects of fluid shear stress. In our previous reports, a hemodynamic lab-on-a-chip system was developed to enable ECs to be subjected to highly precise pulsatile flow. Different fluid shear stresses and glucose concentrations were tested to investigate ROS generation, mitochondrial dysfunction[15] and EC apoptosis[16] under hyperglycaemic conditions. We observed an additive effect of physical and chemical stresses on EC dysfunction under hyperglycaemic conditions, but the influence of other biological factors present in the blood of DM patients remains unclear.

Traditionally, blood components play indispensable roles in vascular function and in most metabolic diseases, including hypocalcaemia, hypoglycaemia, obesity, hyperlipidaemia and metabolic arthritis.[17–21] Hyperglycaemia is the major manifestation of diabetes. However, the vascular complications of diabetes are related to various proteins in the blood and comorbidities inclusive of hyperlipidaemia and hypertension. Low-density lipoprotein (LDL) and high-density lipoprotein (HDL) are two of the five major groups of lipoproteins. LDL concentrations are aggressively reduced in clinical practice to decrease the risk and limit the progression of atherosclerosis, but the importance of increasing HDL has not been well established.[22,23] Meanwhile, how these proteins function under dynamic conditions still remains unknown.

In this paper, we investigate the effect of biological factors in inducing DM-associated EC apoptosis by comparing plasma from healthy volunteers and DM patients in a highly controllable microfluidic system in the presence of multiple apoptosis-inducing factors (Fig. 1A). Pulsatile shear stresses were introduced into the EC surface, and human plasma was mixed with culture medium to simulate the microenvironment of pathological blood including physical, chemical and biological factors. This investigation may help to identify the most prominent cause of EC death in the vascular microenvironment of DM patients, to reveal the interactions among physiological factors in promoting EC apoptosis and to approach the mechanism of how blood components act under dynamic conditions.

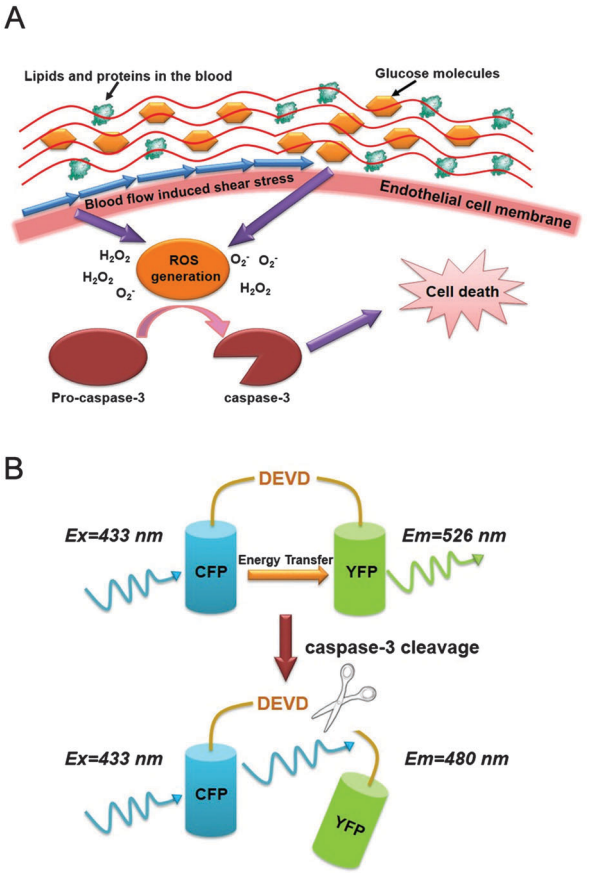

Fig. 1 (A) Schematic illustration of the mechanisms by which blood components and shear stresses induced endothelial cell death, and (B) the principle of a living cell biosensor detecting caspase-3 activation during cell apoptosis based on FRET.

Materials and methods

Construction of endothelial cell with a FRET-based biosensor

In order to detect apoptosis of EC in real-time, human umbilical vein endothelial cells (HUVECs) expressing a fluorescence resonance energy transfer (FRET)-based caspase-3 sensor (HUVEC-C3) were used.[24,25] The FRET sensor was constructed by fusing genes encoding cyan fluorescent protein (CFP), a specific linker containing the caspase-3 cleavage sequence DEVD, and yellow fluorescent protein (YFP) (Fig. 1B). When the cells expressing the FRET sensor are excited with light at the wavelength of CFP (433 nm), the CFP acts as a donor and transfers fluorescence energy to YFP. As a result, the majority of the light is emitted from YFP at 526 nm. When cells undergo apoptosis and caspase-3 is activated, the DEVD sequence linking the CFP and the YFP will be cleaved. This results in the separation of the donor and the acceptor, effectively eliminating the FRET effect. Therefore, when apoptotic cells are excited using the same excitation light as CFP, the majority of light is emitted from CFP at 480 nm. By measuring the fluorescence emission ratio between YFP and

CFP, we can then detect the activation of caspase-3 during apoptosis in real-time.[24] Alternatively, we can determine the apoptotic state of the cells using FRET imaging microscopy. A green colour indicates that the cells are alive, while a blue colour shows that the cells are undergoing apoptosis. The main advantage of this FRET-based biosensor is that no pre- or post-staining is required, enabling direct and convenient detection of apoptosis under *in situ* conditions such as in a microfluidic system.

Protocol for culturing endothelial cells

Normal HUVEC cell line CRL1730 was obtained from ATCC, USA, derived from cells isolated from the umbilical vein. Culture medium was prepared by mixing low glucose (1.0 mg mL^{-1}) DMEM (Gibco, USA) with 10% (v/v) fetal bovine serum (FBS, Hyclone, USA) plus 100 units per mL penicillin and 100 mg mL^{-1} streptomycin (Gibco, USA). HUVECs with a FRET sensor that allows for real-time detection of caspase-3 activation during apoptosis was used (HUVEC-C3).[25] HUVEC-C3 cells were cultured in DMEM medium containing 500 μg mL^{-1} G-418 sulphate (Gibco, USA) to maintain the FRET sensor in the stable cell line. A suspension of cells at a density of approximately 1×10^7 cells per mL was injected into the microchannels, and the microfluidic chip was then incubated in the CO_2 incubator at 37 °C for 48 h until an intact cell monolayer was formed. The monolayer with a constant density of HUVECs will be chosen for further experiments.

The microfluidic experiments were conducted outside of the CO_2 incubator. DMEM with 10 mM HEPES (Sigma, USA) was used to maintain the pH of the culture medium at a physiological value of 7.3–7.4 under atmospheric conditions. A heating platform was used to maintain the temperature of the microfluidic chip and the medium reservoir at 37 °C for long-term circulation of culture medium in the microfluidic system.

Detection of endothelial cell apoptosis *via* the FRET sensor C3

To measure the FRET effect, the microfluidic channels with HUVEC-C3 cell monolayers were excited by a wavelength of 430 ± 10 nm using a fluorescence microscope. The emission images of YFP (530 ± 10 nm) and CFP (480 ± 10 nm) were captured on a computer-controlled CCD camera (Diagnostic Instruments, Inc., USA).[26] The digital fluorescence images of YFP and CTP were merged using ImagePro Plus (Media Cybernetics, USA) to produce FRET images of sensor cells. For each microchannel, multiple observation sites containing at least 200 cells per site were counted and each experiment was conducted in triplicate. The rate of apoptosis was normalised by determining the number of apoptotic cells in blue out of the total number of cells in green and blue.

Detection of endothelial cell death *via* Hoechst staining

Normal HUVEC cells on the Petri dish were pre-treated with Hoechst 33342 (0.5 μg mL^{-1}) and incubated for 20 min. Cells were trypsinized, washed with observation medium and injected into the microchannel in the presence of observation medium. The Hoechst dye molecules can be well maintained by the endothelial cells grown in the microchannel and the fluorescence of these dye molecules will not be affected by the flow of the medium in the microchannel. We compared the fluorescence image of the Hoechst-stained nucleus with the phase image of the ECs, thus verifying that HUVEC-C3 cells were suitable for these experiments.

Hemodynamic lab-on-a-chip system

The hemodynamic lab-on-a-chip system is shown in Fig. 2A. The microfluidic chip was fabricated from polydimethylsiloxane (PDMS) material using standard soft lithography processes.[27] The PDMS slab was bonded to a polylysine coated glass slide (Sigma, USA) by exposure to air plasma for 150 seconds using a handheld corona treater (BD-25, Electro-Technic Products). The microfluidic chip consists of three rows of microchannels that enable triplicate experiments to be performed at the same time. Each row has three different microchannel designs that mimic different blood vessel shapes (Fig. 2B and C), and these microchannels are sites for EC culture. Microchannel design 1 has a width of 600 μm, a height of 150 μm and a total length of 3 cm to mimic normal human arteries. Microchannel design 2 has a width of 600 μm at the beginning of the channel and gradually becomes narrower, reaching 300 μm in the middle of the channel. In microchannel design 3, we introduced a half-circle block with a radius of 300 μm in the middle of the channel to mimic the blood vessel with an atherosclerotic plaque (Fig. 2C). The height and the total length of designs 2 and 3 remain the same as design 1.

According to Poiseuille's equation for calculating the shear stress of a channel with a rectangular shape,[15] $\tau = 12Q\mu/h^2w$, where Q is the volume flow rate, μ is the viscosity of culture medium, which is 1.2 MPa s in our experiments, h is the height of the microchannel at the fixed size of 150 μm, and w is the width of the microchannel. As all three channel designs have the same parameters except for the reduced width in some areas of designs 2 and 3, those channels feature greater shear stresses.

The experimental procedure using the multi-channel microfluidic chip is illustrated in Fig. 2B. This optimised connection of the pulsation-free pump and microfluidic chip allows for a very small amount of medium to circulate in the system and reduces the chance of contamination upon exposure to the environment. Before the introduction of the pulsatile flow, ECs were injected into all the microchannels to form a blood vessel-like monolayer. As shown in Fig. 2B, the two syringes on the pulsation free pump (neMESYS, Cetoni) were connected with three-way valves. Syringe I was used to collect the medium from the medium reservoir. Syringe II was used to inject the medium directly into the microfluidic chip to generate pulsatile flow. Once the two syringes approached their capacities, the two three-way valves were set so as to alter the connection to simultaneously change the flow direction. Consequently, the roles of these two syringes were reversed. In this experimental set-up, the volume of medium circulating in the system and the direction of medium flowing over the endothelial cell monolayer remained the same.

Pulsatile shear stress in the circulation system

In this experiment, two different flow profiles were applied that simulate the actual pulsatile blood flow in the human circulation. One is a pulsatile flow at an average flow rate of 1.41 μL s^{-1}, which produces an average shear stress of 15 dyne per cm^2 in

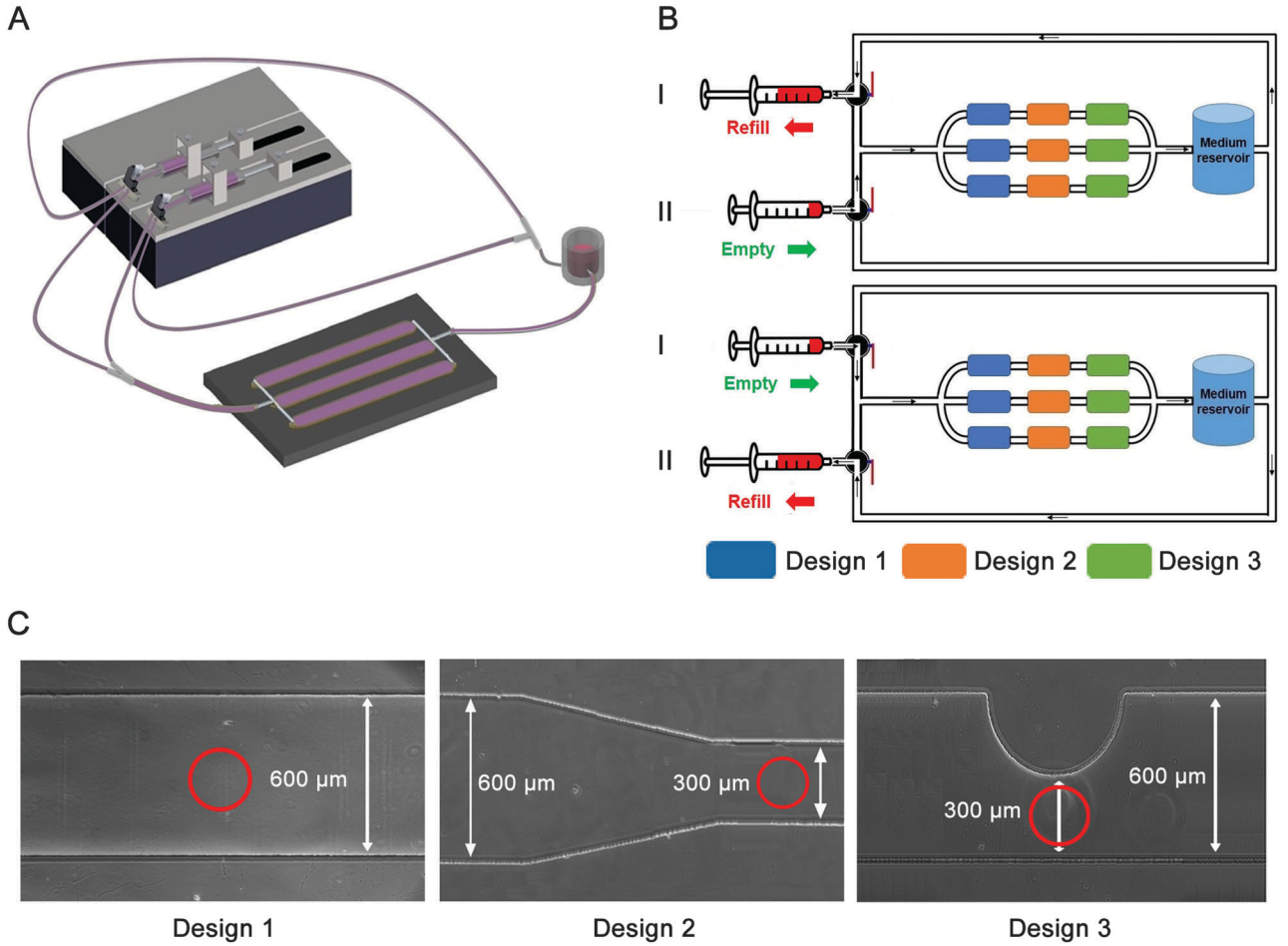

Fig. 2 Design of the microfluidic system. (A) Schematic illustration of the hemodynamic system, (B) flow process and connection method in the experiments, allowing for a very small volume of liquid to circulate in the system, and (C) phase image of microchannel designs 1, 2 and 3 with observation sites circled.

600 μm-wide channels, with a pulse rate of 70 beats per min (bpm). This condition mimics the blood flow in the artery of a healthy human body.[28–30] The other profile is a pulsatile flow at an average flow rate of 2.22 μL s^{-1} with a pulse rate of 110 bpm to simulate the blood flow in DM patients with an increased resting heart rate, resulting in a higher average shear stress of 23.6 dyne per cm^2 in 600 μm-wide channels.[31] The average flow rate was interpreted into the typical flow velocity curve of the artery[15] and imported into neMESYS software. The duration of the flow rate curve was set at 860 ms for 70 bpm and 548 ms for 110 bpm, respectively. As apoptosis is a programmed death event, caspase activation is expected to occur after cells being exposed to the death inducer for certain times. In this experiment, the cells were exposed to the shear stress treatment for 8 h. Afterwards the microfluidic chips were removed from the system and incubated for 40 h in a heating chamber, which maintained a temperature of 37 °C and a similar humidity to that in a CO_2 incubator.

Preparation of plasma from healthy volunteers and DM patients

Plasma samples from three healthy volunteers and six DM patients were obtained from the diabetes and endocrine centre at Tan Tock Seng Hospital. An ethical approval document was obtained from Domain Specific Review Board of National Healthcare Group of Singapore (DSRB, Ref 2012/02218), and all patients signed an informed consent form. All the investigations using human plasma samples were performed under the ethical guidelines and were approved by Biosafety Committee of Nanyang Technological University. The whole blood samples were immediately centrifuged at 4 °C. The supernatant plasma was collected in glass tubes and stored at −20 °C for long-term storage and transportation. The plasma obtained from healthy volunteers was applied as the control group (glucose level considered to be 5 mM) and the plasma from DM patients as the experimental group. The human blood plasma was pre-warmed to 37 °C and mixed with serum free DMEM-HEPES to 10% (v/v). Additional glucose solutions were added to match the glucose level of the medium to the original glucose level of the blood sample. The demographics, physical characteristics and concomitant conditions in healthy volunteers and DM patients are summarised in Tables S1 and S2 (ESI†), respectively.

Inhibition of apoptosis by a pan-caspase inhibitor

To prove that pulsatile shear stress and the plasma samples themselves can induce caspase-dependent apoptosis, the caspase

inhibitor Z-VAD-FMK was used to determine whether it could reduce the rate of EC apoptosis. Before they were subjected to pulsatile flow using DM patients' plasma samples, HUVEC-C3 cells were pre-treated with 40 μM of the pan-caspase inhibitor Z-VAD-FMK for 2 h. Afterwards, cells were treated with culture medium containing DM patient plasma flooded through in a pulsatile manner for 8 h. The apoptotic rate was measured after 40 h of incubation.

Proteomics and western blot analysis

Two-dimensional differential in-gel electrophoresis (2D-DIGE) was performed using Applied Biomics (Hayward, CA, USA) to identify protein biomarkers in the plasma of patients with type 2 diabetes. This study used two plasma samples from patients with glucose levels of 18.8 mM and 12.6 mM and one sample from the healthy volunteer 3. Proteins from each sample were separately labelled with Cy2 (excitation wavelength = 492 nm, emission wavelength = 510 nm), Cy3 (excitation wavelength = 550 nm, emission wavelength = 570 nm), and Cy5 (excitation wavelength = 650 nm, emission wavelength = 670 nm). The labelled proteins from 3 samples were mixed and run on a 2D-DIGE with isoelectric focusing as the first dimension and SDS-PAGE as the second dimension. Fluorescence images were captured using a Typhoon image scanner and analysed using ImageQuant software. The ratio of protein expression between the patient samples and the control sample was quantified using DeCyder software analysis. Proteins that were up-regulated or down-regulated by 1.5-fold with $p \leq 0.05$ compared with the control samples were selected. The protein spots were cut out and subjected to in-gel trypsin digestion followed by protein identification using MALDI-TOF/TOF mass spectrometry using Applied Biomics (Hayward, CA, USA).

To validate the expression levels of biomarkers identified by 2D-DIGE in clinical samples, the plasma containing 100 μg of total protein were separated using 12% SDS-PAGE and transferred onto Amersham Hybond ECL nitrocellulose membranes (GE Healthcare, WI). After blocking the membranes with 5% non-fat milk, the membranes were incubated with primary antibodies from Abcam, UK against haptoglobin, clusterin, apoplipoprotein C-III, and transferrin at 1 : 1000 (v/v) dilutions overnight at 4 °C. The membranes were then incubated with HRP-conjugated secondary antibodies at 1 : 5000 (v/v) dilutions at room temperature for 1 h and developed using an Amersham ECL™ Western-blotting Analysis System (GE Healthcare).

Statistical analysis

All data are presented as the mean ± SD of at least three independent experiments. Statistical significance was analysed using a one-tailed Student's *t* test. Only data with $*p < 0.05$ and $**p < 0.01$ were considered to be significant compared with the control group.

Experimental results and discussion

Higher levels of both glucose and pulsatile shear stress can induce apoptosis in endothelial cells

As we previously showed that high glucose and high shear stress could induce EC apoptosis,[15,16] in this study we examined this issue under conditions that are closer to the clinical situation. Three microchannels with different shapes were designed to generate different flow forces mimicking the blood flow-induced shear stresses in normal, narrowed and partially blocked human arteries (Fig. 2C). Glucose was added to the culture medium to match the blood glucose concentration of each of the six clinical samples (Table S2, ESI†). Pulsatile flow was introduced for 8 h. After incubating cells under static conditions for an additional 40 h, the apoptotic rates of HUVEC-C3 cells were determined by calculating the percentage of apoptotic cells. As shown in Fig. 3, apoptotic cells appeared blue, while live cells appeared green in the FRET images. For each condition, 1000–2000 cells were analysed, and the quantitative data in Fig. 5A showed that a higher glucose concentration induced more EC apoptosis.

Elevating shear stress by reducing channel dimensions significantly increased the rate of apoptosis, especially in cells treated with high glucose concentrations of 15.8–18.8 mM (Fig. 5A). For example, for cells treated with 18.8 mM glucose, the percentage of apoptosis increased sharply from 16.7% to 24.9% and 40.4% for channels 1, 2, and 3, respectively. In contrast, for cells treated with 12.4 mM glucose, the rate of apoptosis only increased slightly from 9.8 to 11.6% (Fig. 5A). In addition to using FRET imaging to indicate caspase-3 activation, cells were stained with the DNA dye Hoechst 33342 as an apoptotic indicator measuring chromatin condensation and DNA fragmentation. A similar level of apoptosis was detected using this method (Fig. S1, ESI†). These results suggest that increasing shear stress is much more harmful to ECs at a high glucose concentration than it is at a low glucose concentration.

More importantly, under static conditions, treating cells with 18.8 mM glucose medium for 48 h only induced 7.32% HUVEC-C3 cells to undergo apoptosis, which is 5.5-fold less effective than the pulsatile flow achieved in microchannel design 3. This observation further demonstrates the critical role of pulsatile shear stress in driving hyperglycaemia-induced EC death. This result indicates the combined effects of the physical force of shear stress and the chemical factor of high glucose in causing additive damage to the endothelium lining the inner layer of blood vessels in DM patients.

Plasma from DM patients induced more cells to undergo apoptosis compared to medium with the same glucose concentration

Hyperglycaemia has been considered as a hallmark of diabetes. However, in the microenvironment of blood vessels, blood components including proteins, lipids and antioxidant vitamins should serve as factors protecting or damaging the endothelium. From this perspective, we combined clinically obtained plasma with the microfluidic system to investigate how these biological factors function in an experimental set up with pulsatile shear stress and hyperglycaemia. The experimental conditions were identical to those used with glucose medium, with the exception that 10% plasma from either healthy volunteers or DM patients was replaced with FBS.

We measured the rates of EC apoptosis in three different channel designs when exposed to the plasma of six DM patients

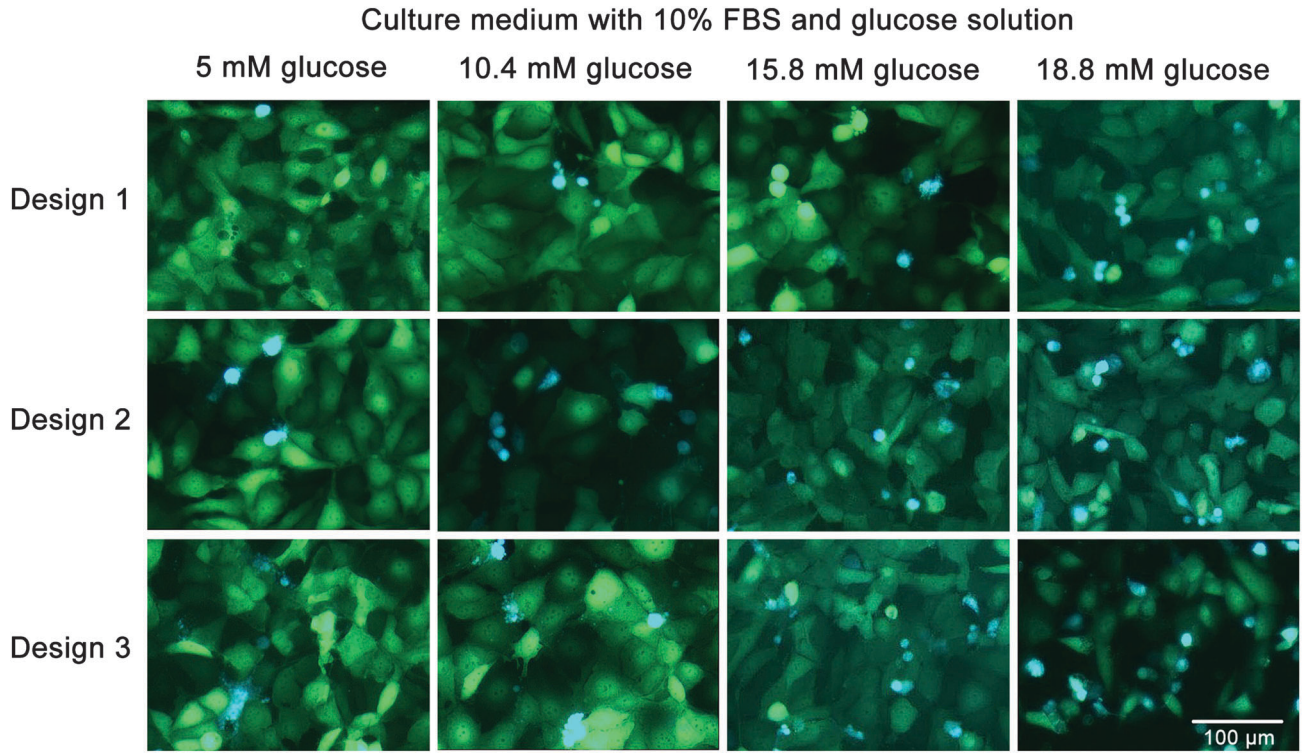

Fig. 3 Merged images of HUVEC-C3 cells with FRET effects under different glucose concentrations and different microchannel designs using medium with 10% FBS and defined glucose concentrations.

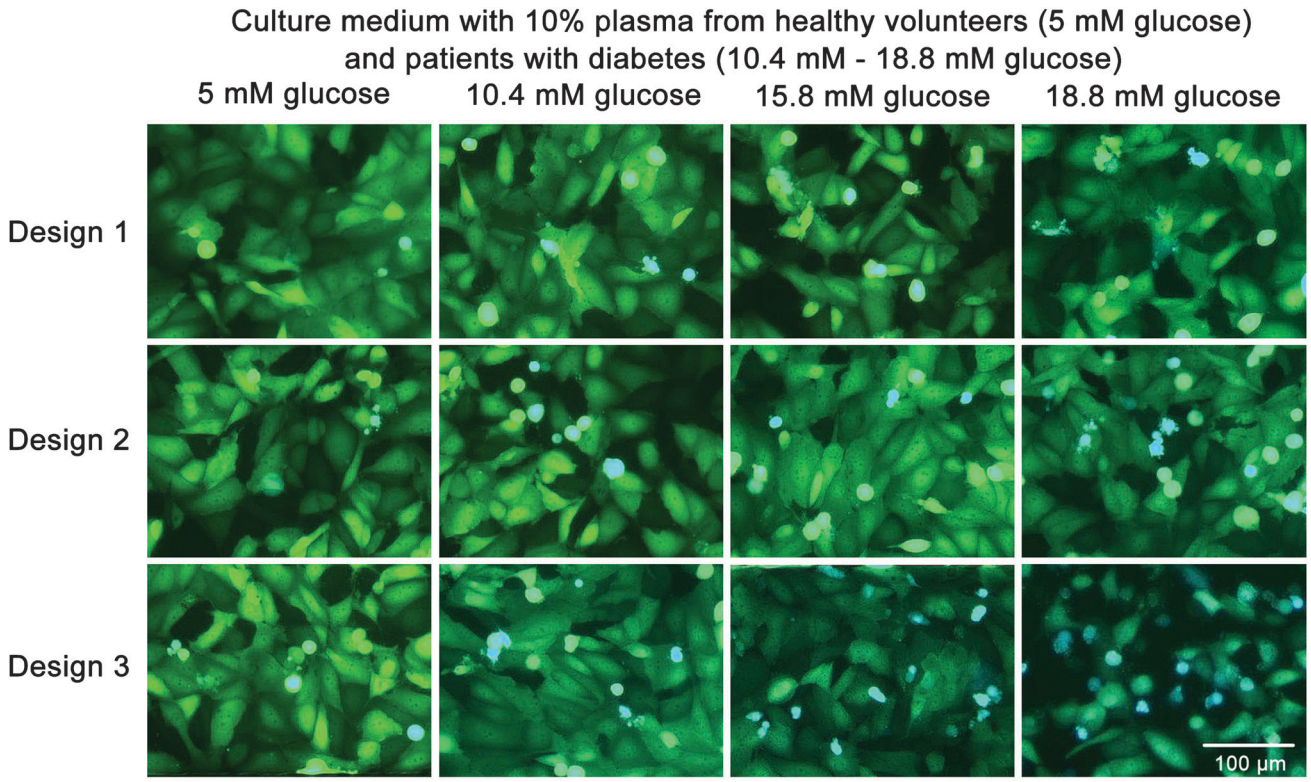

Fig. 4 Merged images of HUVEC-C3 cells with FRET effects in different microchannel designs using medium with 10% plasma from healthy volunteers or DM patients at defined glucose concentrations.

or three healthy volunteers. Fig. 4 presents representative FRET images from three different microchannel designs at four glucose concentrations. Fig. 5B presents the results of quantitative analysis of 1000–2000 cells under each experimental condition. Although we observed that a higher glucose concentration significantly increased the rate of apoptosis as observed in the glucose medium experiment shown in Fig. 5A, much higher levels of apoptosis were detected in cells treated with the high glucose patient's plasma compared with cells treated with glucose medium under the lower shear stress situation generated in channel designs 1 and 2 (Fig. 5A and B). In these cases, the rate of apoptosis was 1.4–2.3 times higher for the patient's plasma compared with the FBS medium containing the same concentration of glucose (Table 1). The additive apoptotic effect was not observed either for cells seeded in microchannel 3, in which the higher shear stress already induced a high level of apoptosis, or for cells in the static condition (Fig. 5 and Table 1).

The results obtained from human plasma suggest that other components of patients' plasma besides glucose can further damage ECs. These components can even carry out their harmful effects on ECs in microchannel designs 1 and 2, representing normal and the gradually narrowed blood vessels present in

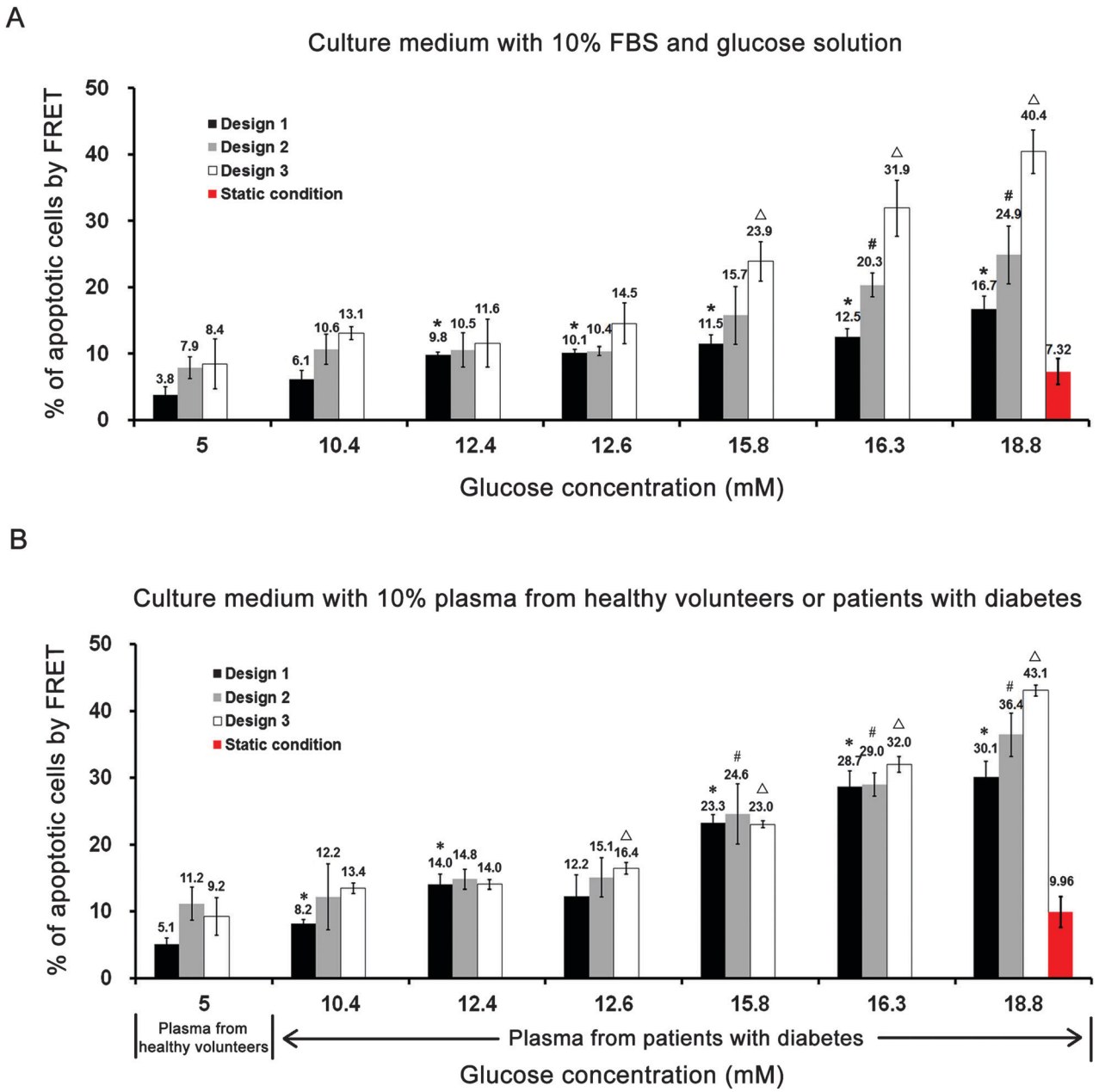

Fig. 5 The percentage of apoptotic cells was determined by analysing 1000–2000 cells in the merged FRET images for each condition. (A) Medium with 10% FBS and glucose concentrations equivalent to the clinical samples, and (B) 10% plasma of healthy volunteers and type 2 DM patients ($p < 0.05$ compared to the first group in all samples of A or B in microchannel design 1*, design 2$^{\#}$ and design 3$^{\Delta}$, respectively).

Table 1 Ratio of rate of apoptosis between DM patients' plasma and medium with FBS

Glucose concentration (mM)	Microchannel design	Apoptotic rate – DM plasma	Apoptotic rate – FBS medium	Ratio of DM plasma/FBS
15.8	1	23.3	11.5	2.0
	2	24.6	15.7	1.6
	3	23.0	23.9	1.0
16.3	1	28.7	12.5	2.3
	2	29.0	20.3	1.4
	3	32.0	31.9	1.0
18.8	1	30.1	16.7	1.8
	2	36.4	24.9	1.5
	3	43.1	40.4	1.1

most patients with diabetes. As EC dysfunction can lead to many diabetes-related vascular diseases, the identities of these components should be investigated.

A sudden increase in shear stress induces more apoptosis in endothelial cells, which can be reduced by a caspase inhibitor

Before finding the pro-apoptotic factors in the plasma samples, we investigated the impact of sudden changes in the shear stresses applied to ECs. The shear stresses at the observation sites in microchannel designs 2 and 3 were the same but induced different rates of EC apoptosis. This finding indicates that in the human body, pathological plaques possess a higher risk of causing endothelial destruction and ulceration. To further investigate the impact of this sudden change, the rates of apoptosis of HUVEC-C3 cells were compared between the observation site and its upstream or downstream site within the same microchannel (Fig. 6A). The experiment was conducted using the same conditions described above using the DM patient's sample with 18.8 mM glucose. Merged images of FRET effects are shown in Fig. 6B.

The bar graph in Fig. 6C shows that 43.1% of HUVEC-C3 cells underwent apoptosis in the observation site at the point where the channel diameter suddenly decreases from 600 to 300 μm. A much lower rate of apoptosis of approximately 29% was found in areas either upstream or downstream of the partially blocked site, similar to the rate of 30.1% observed using the plasma sample with 18.8 mM glucose in microchannel design 1 (Fig. 5B). This finding suggests that the sudden change in shear stress can damage the ECs directly exposed to these flow forces, but will not affect the ECs in the surrounding areas.

The pan-caspase inhibitor Z-VAD-FMK was used to determine whether this multi-factor-induced apoptosis could be reduced by inhibiting caspase-3 activation. HUVEC-C3 cells were pre-treated with 40 μM of the pan-caspase inhibitor Z-VAD-FMK for 2 h and exposed to the flow of a plasma sample with 18.8 mM glucose. This result shows that the percentage of EC apoptosis was reduced from 43.1% to 24.1% (Fig. 6D). This result confirms that EC apoptosis can occur under pulsatile shear stresses and the biochemical conditions present in the clinical plasma samples. Furthermore, it also suggests that preventing caspase activation could be a therapeutic strategy for treating diabetic vascular complications by reducing EC apoptosis.

Identification of proteins with an altered expression profile in the plasma of DM patients

Little difference in cell death was observed between the glucose medium and patients' plasma in microchannel design 3. One possible reason for this is that the mechanical forces of the high flow rate reduced the interaction between plasma proteins and the endothelium. In this situation, the reduction in the interactions of "bad" proteins and thus their subsequent negative effects was greater than that of "good" proteins, resulting in a smaller increase in the rate of apoptosis of ECs.

To further investigate the biological factors of human plasma that can contribute to EC apoptosis under pathological conditions, we identified these plasma components by comparing the protein profiles between different samples. Proteins in the control plasma from a healthy volunteer were conjugated with Cy2 dye, which emits green fluorescence; proteins in the DM patient plasma with a glucose concentration of 12.6 mM were conjugated with Cy3 dye, which emits red fluorescence; and proteins of the DM patient plasma with a glucose concentration of 18.8 mM were conjugated with Cy5 dye, which emits far-red-fluorescence. Three groups of samples were prepared by mixing equal amounts of proteins from each plasma sample: (1) control *vs.* patient 3 with 12.6 mM glucose, (2) control *vs.* patient 5 with 18.8 mM glucose, and (3) patient 3 with 12.6 mM glucose *vs.* patient 5 with 18.8 mM glucose. The proteins in each group of samples were separated by 2D-DIGE based on their electrical charges and molecular weights. Fluorescence images of 2D-DIGE from the first two combinations of three dyes were merged to produce the images in Fig. 7A.

In these merged images, red colour indicates up-regulated proteins, green represents down-regulated proteins, and yellow indicates equivalent expression between the patient and control samples. A total of 76 protein spots could be visualised in the merged images. The fluorescence intensity of each protein spot was quantified by DeCyder analysis. Out of 76 protein spots, the expression levels of 18 were consistently up-regulated or down-regulated at least 1.5-fold with $p \leq 0.05$ among all three groups: (1) 18.8 mM glucose/control, (2) 12.6 mM glucose/control, and (3) 18.8 mM glucose/12.6 mM glucose. These proteins were cut out and subjected to in-gel trypsin digestion followed by protein identification using MALDI-TOF/TOF mass spectrometry using Applied Biomics (Hayward, CA, USA).

Among the 18 identified protein spots listed in Table 2, 12 were differentially down-regulated and the other 6 were up-regulated. Among the 12 down-regulated protein spots, several were found to be the same protein that was separated by 2D-DIGE due to its different pI values. Specifically, proteins at spots 62–64 were all identified to be haptoglobin α2, proteins at spots 32 and 33 were both identified as haptoglobin β, and proteins at spots 37 and 38 were found to be clusterin.

Western blot analysis was used to validate the expression profiles of three representative proteins determined by 2D-DIGE, and positive confirmation was obtained for all three cases (Fig. 7B and C). Both methods revealed that the levels of haptoglobin β and clusterin were reduced more significantly

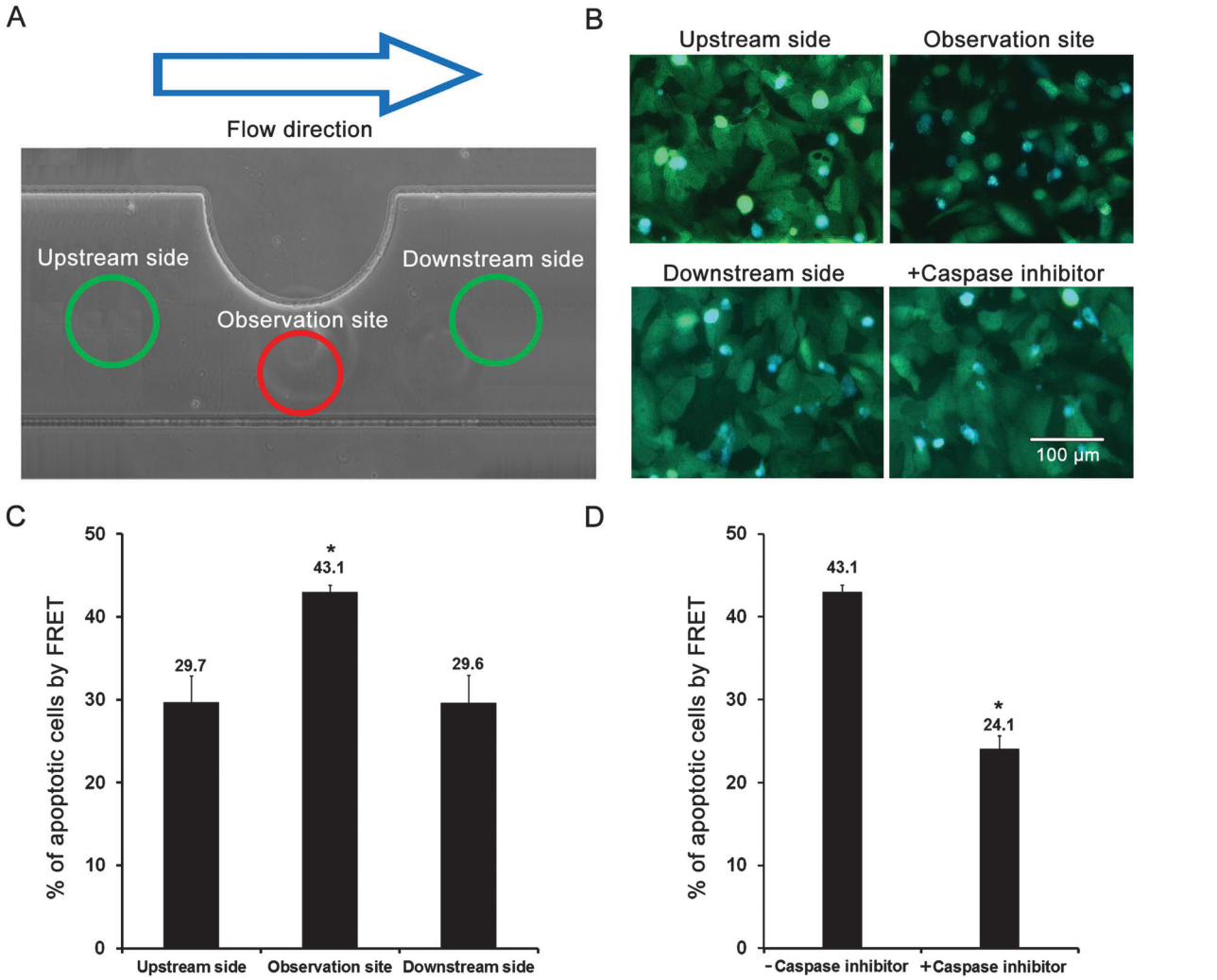

Fig. 6 (A) Illustration of the observation site in microchannel design 3, (B) merged images of HUVEC-C3 cells with FRET effects of different sites of microchannel design 3 in the presence of caspase inhibitor in the DM patient's plasma with 18.8 mM glucose, (C) the percentage of apoptotic cells determined by analysing 1000–2000 cells from the merged FRET images at each site (*$p < 0.05$ compared to the site before or after blocking along the flow direction), and (D) the percentage of apoptotic cells determined by analysing 1000–2000 cells in the merged FRET images with caspase inhibitor treatment (*$p < 0.05$ compared to the observation site).

in the patient plasma with 18.8 mM glucose than in plasma with an intermediate level of glucose at 12.6 mM. Meanwhile, the level of apolipoprotein (Apo) C-III increased more prominently in patient samples with higher glucose.

After examining the functions of the proteins identified here, we realised that all eight proteins with beneficial effects on EC or vascular function were down-regulated, while another six proteins with harmful potential were up-regulated in the plasma of DM patients with hyperglycaemia. For example, the levels of two subunits of haptoglobin (β and α2), with the function of binding and removing haemoglobin from the blood to reduce its oxidative stress were significantly decreased in DM patient's plasma with 18.8 mM glucose, while the level of "bad" haemoglobin β was considerably higher in the DM patient's plasma with higher glucose.

Other examples are the "good" proteins including clusterin, which can promote cell–cell adhesion and inhibit apoptosis by interacting with activated Bax,[32] and the high density lipoproteins of Apo A-I and E, which can remove cholesterol from the blood, were all reduced in hyperglycaemia plasma. The "bad" proteins were present at higher levels in the DM patient's plasma with 18.8 mM glucose, including the low-density lipoproteins Apo C-II and C-III, which can promote the formation of atherosclerotic plaques.

Apolipoprotein C-III is a major component of the family of triglyceride rich lipoproteins. Apo C-III is elevated in metabolic syndrome and DM type 2 and correlates with BMI (Body Mass Index) and insulin sensitivity.[33] The concentration of Apo B with respect to that of Apo C-III is the strongest lipoprotein predictor of the progression of coronary atherosclerosis, even in patients where LDL-cholesterol (LDL-C) was aggressively lowered with lovastatin.[34] Apo C-III in high density lipoprotein-cholesterol (HDL-C) is also associated with coronary heart disease and exhibits a positive correlation with very low density lipoprotein (VLDL) and triglycerides. This suggests that Apo C-III exerts atherogenic properties beyond its effect on Apo B lipoprotein metabolism.[35] Apo C-III alone

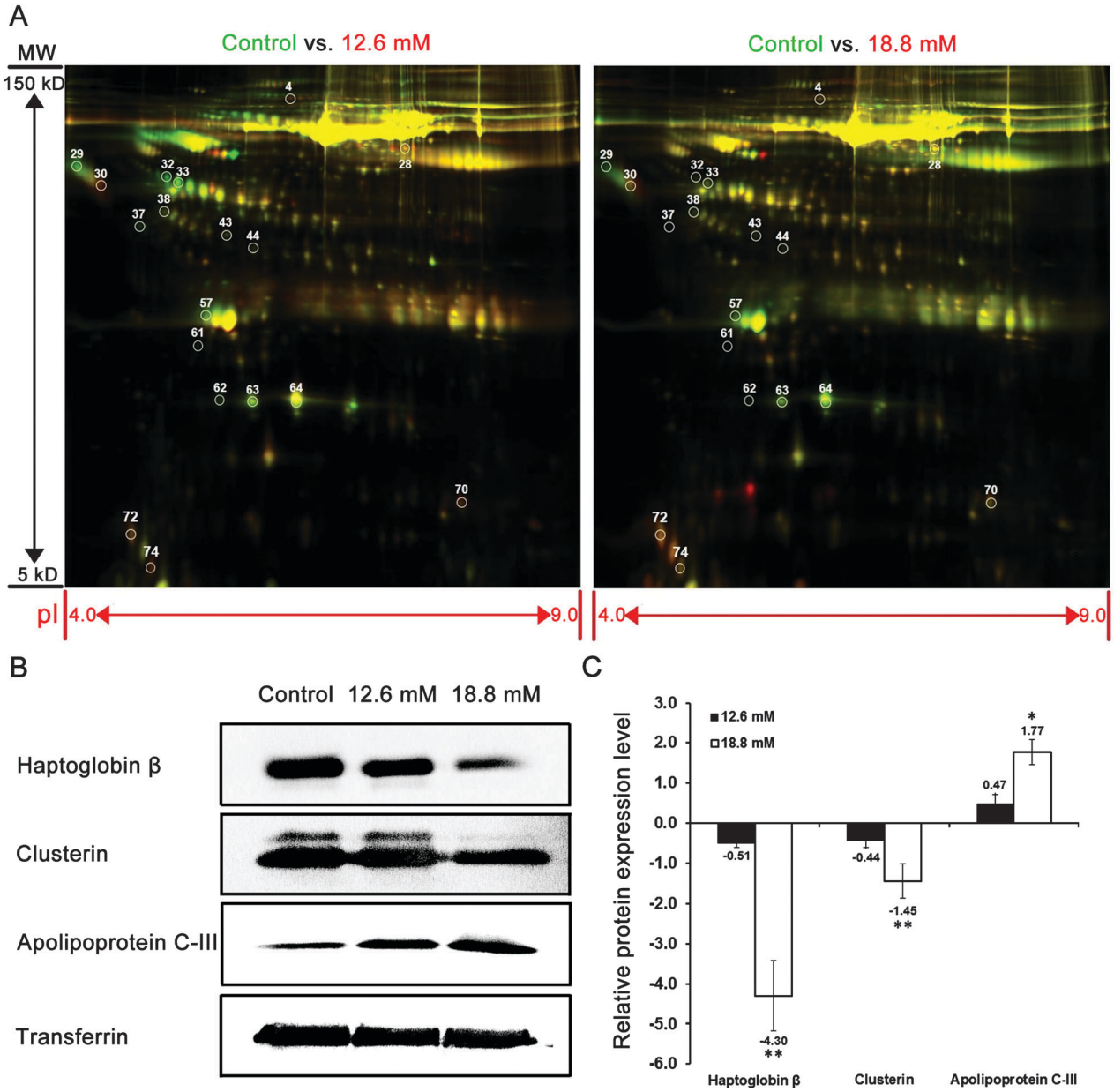

Fig. 7 (A) Fluorescence images of 2D-DIGE with over-expressed proteins in DM patients' plasma compared to healthy volunteer's plasma in red and under expressed proteins in green, (B) western blot analysis of the expression level of haptoglobin, clusterin and apolipoprotein C-III in three of the plasma samples, and (C) histogram of normalised protein levels of the three plasma samples (*$p < 0.05$ and **$p < 0.01$ compared to the group using the DM patient's plasma with a glucose concentration of 12.6 mM).

and Apo C-III rich VLDL increase monocyte adhesion to vascular endothelial cells and activate NF-κB, thus leading to endothelial activation. Apo C-III HDL does not reduce the adhesion of monocytes to vascular endothelial cells, whereas HDL-C with no Apo C-III reduces monocyte adherence, thus counteracting the benefit of HDL-C.[36]

Haptoglobin is known to provide protection against haemoglobin peroxidation-triggered endothelial damage as both the intrinsic haemoglobin oxidation pathway (which generates toxic reaction products causing EC apoptosis) and extrinsic oxidation pathway (which generates lipid oxidation products) can be prevented in the presence of haptoglobin.[37] The lack of haptoglobin is also known to be associated with unbalanced VEGF-alpha/angiopoietin-1 expression, intramural haemorrhage and impaired wound healing after myocardial infarction.[38] Haptoglobin genotypes are also known to be associated with endothelial dysfunction and vascular complications, with haptoglobin genotype 2–2 associated with higher oxidative risk.[39]

Clusterin has also been implicated in lipid metabolism and atherogenesis and is known to be protective. In fact, laminar shear stress is known to up-regulate clusterin, the complement-inhibitory protein, thus preventing endothelial activation through the complement cascade.[40] In a study conducted in hypertensive Japanese women, polymorphisms in the clusterin

Table 2 Information about proteins identified by 2D-DIGE

Spot ID	Protein name	Ratio of protein levels 18.8/C	12.6/C	18.8/12.6	Biological function
29	Alpha-1-acid glycoprotein 2	−28.4	−4.5	−6.1	Carrier of charged lipophilic compounds
57	Apolipoprotein A-I	−5.6	−2.2	−2.4	High-density lipoprotein
43	Apolipoprotein E	−4.4	−2.3	−1.9	High-density lipoprotein
37	Clusterin	−15.4	−8.3	−1.8	Inhibiting apoptosis
38	Clusterin	−3.4	−1.9	−1.7	
32	Haptoglobin β	−22.4	−13.4	−1.6	Binding to free haemoglobin to inhibit oxidative stress
33	Haptoglobin β	−9.8	−6.0	−1.6	
62	Haptoglobin α2	−10.2	−4.0	−2.4	
63	Haptoglobin α2	−5.2	−2.2	−2.2	
64	Haptoglobin α2	−4.0	−1.5	−2.5	
44	Histidine-rich glycoprotein	−4.0	−1.8	−2.1	Modulating immune and vascular system
61	Retinol-binding protein 4	−6.5	−4.2	−1.5	Delivering retinol to liver
30	Alpha-1-acid glycoprotein 2	4.3	3.1	1.5	Carrier of charged lipophilic compounds
74	Apolipoprotein C-II	5.4	2.8	2.0	Very-low-density lipoprotein
72	Apolipoprotein C-III	4.4	1.6	2.9	Very-low-density lipoprotein
28	Beta-2-glycoprotein	2.6	1.6	1.7	Inhibiting coagulation factors
70	Haemoglobin β subunit	8.1	4.6	1.8	Inducing oxidative stress
4	Serum albumin	2.1	1.5	1.5	Transporting hormones, fatty acids

gene influenced lipid levels and the thickness of the carotid intima media.[41]

In one study, proteomic analyses of HDL-C from patients with coronary artery disease were compared to those of healthy individuals. HDL proteomic analyses and subsequent validation and functional characterisation suggested a reduced clusterin and increased Apo C-III content of HDL-C in patients with coronary artery disease when compared to normal individuals as mechanisms leading to altered effects on endothelial apoptosis.[42]

In summary, this study established a positive correlation among protein expression profiles, glucose level, and apoptosis induction. The plasma of the DM patient with 18.8 mM glucose had an elevated level of proteins with negative functions (1.5–2.9-fold increase) and a reduced level of proteins with positive functions (1.5 to 6.1-fold reduction) compared with the plasma with 12.6 mM glucose (Table 2). The plasma with 18.8 mM glucose also induced a much higher level of apoptosis (30.1% to 43.1% for channel designs 1–3) than the plasma with 12.6 mM glucose (12.2% to 16.4% for channel design 1–3) (Fig. 5B).

Conclusions

In this paper, we investigated the harmful effects of the pathological microenvironment inside the bloodstream of DM patients upon the induction of EC apoptosis. With the aid of HUVEC-C3 sensor cells, the transition from live to dead cells could be non-invasively determined in real-time by visualising the colour changes of cells from green to blue. A hemodynamic lab-on-a-chip system was used to generate fluid shear stress simulating the pulsatile flow of the bloodstream at different flow and pulse rates. The sizes and shapes of microchannels were engineered to mimic the normal, narrowed or partially blocked blood vessels representing healthy or damaged blood vessels with increased shear stress. Plasma with various concentrations of blood glucose was obtained from DM patients and healthy volunteers and used to investigate the apoptotic effects of glucose and plasma components on EC. The results showed that more ECs underwent apoptosis if they encountered higher levels of physical factor of pulsatile shear stress or higher levels of chemical factor of glucose. The most important finding of this study is that in addition to hyperglycaemia, other plasma components can also contribute to additional EC apoptosis. By analysing the expression profiles of plasma samples, we identified fourteen proteins including apolipoprotein C-III, haemoglobin β, haptoglobin, and clusterin, and the expression levels of these proteins were significantly altered in agreement with the concentration of blood glucose and the ability to stimulate apoptosis. If the expression profiles of these proteins can be validated using large numbers of patient samples, then the plasma levels of those proteins may serve as new indicators predicting the level of endothelial dysfunction in the arteries of DM patients, thus enabling clinical evaluation of the risk of vascular complications.

Acknowledgements

This work was supported in part by the Singapore National Research Foundation NRF-CRP8-2011-05 (Grant No. M4092018.0S4), the Ministry of Education of Singapore AcRF Tier 1 (Grant No. M4010891.120), and the Environmental and Water Industry Development Council of Singapore (Grant No. 1102-IRIS-05-02).

References

1 T. Jensen and T. Deckert, *Horm. Metab. Res., Suppl. Ser.*, 1992, **26**, 68–70.
2 J. A. Beckman, M. A. Creager and P. Libby, *JAMA, J. Am. Med. Assoc.*, 2002, **287**, 2570–2581.
3 P. Vallance, A. Calver and J. Collier, *J. Hypertens. Suppl.*, 1992, **10**, S25–S29.
4 A. A. Quyyumi, *Am. J. Med.*, 1998, **105**, 32S–39S.
5 Y. Takamura, T. Tomomatsu, E. Kubo, S. Tsuzuki and Y. Akagi, *Invest. Ophthalmol. Visual Sci.*, 2008, **49**, 3216–3223.
6 M. L. Sheu, C. K. Chiang, K. S. Tsai, F. M. Ho, T. I. Weng, H. Y. Wu and S. H. Liu, *Free Radical Biol. Med.*, 2008, **44**, 2043–2050.
7 N. Das Evcimen and G. L. King, *Pharmacol. Res.*, 2007, **55**, 498–510.
8 L. Quagliaro, L. Piconi, R. Assaloni, L. Martinelli, E. Motz and A. Ceriello, *Diabetes*, 2003, **52**, 2795–2804.
9 S. Srinivasan, M. E. Hatley, D. T. Bolick, L. A. Palmer, D. Edelstein, M. Brownlee and C. C. Hedrick, *Diabetologia*, 2004, **47**, 1727–1734.
10 M. Papadaki, S. G. Eskin, J. Ruef, M. S. Runge and L. V. McIntire, *Diabetes Res. Clin. Pract.*, 1999, **45**, 89–99.
11 N. Resnick, H. Yahav, A. Shay-Salit, M. Shushy, S. Schubert, L. C. Zilberman and E. Wofovitz, *Prog. Biophys. Mol. Biol.*, 2003, **81**, 177–199.
12 O. Tricot, Z. Mallat, C. Heymes, J. Belmin, G. Leseche and A. Tedgui, *Circulation*, 2000, **101**, 2450–2453.
13 C. G. Galbraith, R. Skalak and S. Chien, *Cell Motil. Cytoskeleton*, 1998, **40**, 317–330.
14 P. F. Davies, *Physiol. Rev.*, 1995, **75**, 519–560.
15 L. K. Chin, J. Q. Yu, Y. Fu, T. Yu, A. Q. Liu and K. Q. Luo, *Lab Chip*, 2011, **11**, 1856–1863.
16 J. Q. Yu, X. F. Liu, L. K. Chin, A. Q. Liu and K. Q. Luo, *Lab Chip*, 2013, **13**, 2693–2700.
17 C. M. Armstrong and G. Cota, *Proc. Natl. Acad. Sci. U. S. A.*, 1999, **96**, 4154–4157.
18 P. E. Cryer, L. Axelrod, A. B. Grossman, S. R. Heller, V. M. Montori, E. R. Seaquist and F. J. Service, *J. Clin. Endocrinol. Metab.*, 2009, **94**, 709–728.
19 L. A. Barness, J. M. Opitz and E. Gilbert-Barness, *Am. J. Med. Genet., Part A*, 2007, **143A**, 3016–3034.
20 A. Chait and J. D. Brunzell, *Endocrinol. Metab. Clin. North Am.*, 1990, **19**, 259–278.
21 G. Nuki and P. A. Simkin, *Arthritis Res. Ther.*, 2006, 8.
22 R. Stocker and J. F. Keaney, Jr., *Physiol. Rev.*, 2004, **84**, 1381–1478.
23 R. M. Krauss, *Curr. Opin. Lipidol.*, 2010, **21**, 305–311.
24 K. Q. Luo, V. C. Yu, Y. Pu and D. C. Chang, *Biochem. Biophys. Res. Commun.*, 2001, **283**, 1054–1060.
25 X. Zhu, A. Fu and K. Q. Luo, *Biochem. Biophys. Res. Commun.*, 2012, **418**, 641–646.
26 H. Tian, L. Ip, H. Luo, D. C. Chang and K. Q. Luo, *Br. J. Pharmacol.*, 2007, **150**, 321–334.
27 L. K. Chin, A. Q. Liu, Y. C. Soh, C. S. Lim and C. L. Lin, *Lab Chip*, 2010, **10**, 1072–1078.
28 D. N. Ku, *Annu. Rev. Fluid Mech.*, 1997, **29**, 399–434.
29 X. He, D. N. Ku and J. E. Moore, Jr., *Ann. Biomed. Eng.*, 1993, **21**, 45–49.
30 D. J. Duncker and R. J. Bache, *Physiol. Rev.*, 2008, **88**, 1009–1086.
31 G. S. Hillis, J. Hata, M. Woodward, V. Perkovic, H. Arima, C. K. Chow, S. Zoungas, A. Patel, N. R. Poulter, G. Mancia, B. Williams and J. Chalmers, *J. Am. Heart Assoc.*, 2012, **1**, e002832.
32 A. Z. Badros, O. Goloubeva, A. P. Rapoport, B. Ratterree, N. Gahres, B. Meisenberg, N. Takebe, M. Heyman, J. Zwiebel, H. Streicher, C. D. Gocke, D. Tomic, J. A. Flaws, B. Zhang and R. G. Fenton, *J. Clin. Oncol.*, 2005, **23**, 4089–4099.
33 O. Olivieri, A. Bassi, C. Stranieri, E. Trabetti, N. Martinelli, F. Pizzolo, D. Girelli, S. Friso, P. F. Pignatti and R. Corrocher, *J. Lipid Res.*, 2003, **44**, 2374–2381.
34 P. Alaupovic, W. J. Mack, C. Knight-Gibson and H. N. Hodis, *Arterioscler., Thromb., Vasc. Biol.*, 1997, **17**, 715–722.
35 A. Onat, G. Hergenc, V. Sansoy, M. Fobker, K. Ceyhan, S. Toprak and G. Assmann, *Atherosclerosis*, 2003, **168**, 81–89.
36 A. Kawakami and M. Yoshida, *J. Atheroscler. Thromb.*, 2009, **16**, 6–11.
37 C. A. Schaer, J. W. Deuel, A. G. Bittermann, I. G. Rubio, G. Schoedon, D. R. Spahn, R. A. Wepf, F. Vallelian and D. J. Schaer, *Cell Death Differ.*, 2013, **20**, 1569–1579.
38 F. Arslan, M. B. Smeets, B. Buttari, E. Profumo, R. Rigano, L. Akeroyd, E. Kara, L. Timmers, J. P. Sluijter, B. van Middelaar, K. den Ouden, G. Pasterkamp, S. K. Lim and D. P. de Kleijn, *J. Mol. Cell. Cardiol.*, 2013, **56**, 116–128.
39 M. Vardi and A. P. Levy, *Curr. Diabetes Rep.*, 2012, **12**, 274–279.
40 C. Urbich, M. Fritzenwanger, A. M. Zeiher and S. Dimmeler, *Circulation*, 2000, **101**, 352–355.
41 Y. Miwa, S. Takiuchi, K. Kamide, M. Yoshii, T. Horio, C. Tanaka, M. Banno, T. Miyata, T. Sasaguri and Y. Kawano, *Biochem. Biophys. Res. Commun.*, 2005, **331**, 1587–1593.
42 M. Riwanto, L. Rohrer, B. Roschitzki, C. Besler, P. Mocharla, M. Mueller, D. Perisa, K. Heinrich, L. Altwegg, A. von Eckardstein, T. F. Luscher and U. Landmesser, *Circulation*, 2013, **127**, 891–904.

